STRUCTURAL AND CHEMICAL CONTRASTS BETWEEN PRISMATIC AND FIBROUS FLUORO-EDENITE FROM BIANCAVILLA, SICILY, ITALY

Antonio GIANFAGNA[§], Giovanni B. ANDREOZZI, Paolo BALLIRANO
AND Simona MAZZIOTTI-TAGLIANI

*Dipartimento di Scienze della Terra, Università degli Studi di Roma "La Sapienza",
Piazzale A. Moro, 5, I–00185 Rome, Italy*

Biagio M. BRUNI

Dipartimento Tecnologie e Salute, Istituto Superiore di Sanità, Viale Regina Elena, 299 , I–00162 Rome, Italy

ABSTRACT

Fluoro-edenite [$NaCa_2Mg_5(Si_7Al)O_{22}F_2$], a new end-member of the calcic amphibole group, is present with both prismatic and fibrous morphologies in the altered volcanic products of the Monte Calvario locality, Biancavilla, on the flanks of Mount Etna, Sicily, Italy. Whereas the crystal chemistry of the prismatic variety was described recently, the fibrous variety has not been well characterized. We report original crystal-chemical and structural data on this fibrous amphibole. Because of the difficulty in analyzing this micrometric material, specific procedures of sample preparation were developed. SEM–EDS microanalyses and Mössbauer spectroscopy indicate a variable composition of the fibers, ranging mostly from fluoro-edenite to, subordinately, winchite, tremolite, and richterite compositions. Given the impossibility of using a single-crystal X-ray method, the powder-diffraction data were evaluated by the Rietveld method. By combining the microchemical data, Mössbauer Fe^{3+}/Fe_{tot} values, and with a refinement of the structure, the following chemical formula was obtained from an averaged composition of all the fibrous amphibole analyzed: $(Na_{0.307}K_{0.157})_{\Sigma0.464} (Ca_{1.505}Na_{0.495})_{\Sigma2.000} (^{VI}Al_{0.104}Fe^{3+}_{0.333}Fe^{2+}_{0.162}Mg_{4.255}Ti_{0.062}Mn_{0.063})_{\Sigma4.980}$ $(Si_{7.520}{}^{IV}Al_{0.480})_{\Sigma8.000} O_{22} (F_{1.970}Cl_{0.020})_{\Sigma1.990}$. The cell parameters, positional parameters for all the atoms, and site scattering for O3, $M1$, $M2$, $M3$, $M4$, A, and $A(m)$ were refined. In agreement with the site occupancies of cations based on both XRPD and Mössbauer data, Fe^{2+} was assigned to the $M2$ and $M3$ sites, and all Fe^{3+} was assigned to the $M2$ site. In particular, Fe^{2+} content of each $M2$ site is far greater (0.125 *apfu*) than that of $M3$ (0.037 *apfu*). The analytical procedures utilized here can be adopted for all types of mineral fibers, whether they belong to the asbestiform group of amphiboles or not. In addition to their mineralogical interest, these results are also relevant for environmental and health aspects. The interactions between mineral fiber and the biological environment are strongly related to the crystal chemistry of the fibrous materials.

Key words: fibrous Ca-amphiboles, fluoro-edenite, Mössbauer spectroscopy, Rietveld method, EDS micro-analyses, crystal chemistry, Etna volcano, Biancavilla, Italy.

SOMMAIRE

La fluoro-édenite [$NaCa_2Mg_5(Si_7Al)O_{22}F_2$], nouveau pôle parmi les amphiboles calciques, est présente sous forme de prismes et de fibres dans les produits volcaniques altérés de Monte Calvario, à Biancavilla, sur les flancs du mont Etna, en Sicile, Italie. Quoique la chimie cristalline de la variété prismatique a été décrite récemment, la variété fibreuse demeure méconnue. Nous présentons des données originales sur les aspects cristallochimiques et structuraux de cette amphibole fibreuse. A cause de difficultés à analyser ce matériau micrométrique, nous avons dû développer des procédures spécifiques pour la préparation d'échantillons. Les analyses faites au microscope électronique à balayage en dispersion d'énergie et par spectroscopie de Mössbauer indiquent une composition variable des fibres, correspondant surtout à la fluoro-édenite mais aussi, en quantités moindres, à la winchite, la trémolite, et la richterite. A cause de l'impossibilité d'utiliser la diffraction X sur monocristal, nous avons utilisé la méthode de Rietveld et les données en diffraction X obtenues sur poudre. D'après une combinaison des données microchimiques, les valeurs de Fe^{3+}/Fe_{tot} résultant des spectres de Mössbauer, et un affinement de la structure, nous obtenons la formule chimique moyenne suivante pour décrire l'amphibole fibreuse analysée: $(Na_{0.307}K_{0.157})_{\Sigma0.464} (Ca_{1.505}Na_{0.495})_{\Sigma2.000}$ $(^{VI}Al_{0.104}Fe^{3+}_{0.333}Fe^{2+}_{0.162}Mg_{4.255}Ti_{0.062}Mn_{0.063})_{\Sigma4.980} (Si_{7.520}{}^{IV}Al_{0.480})_{\Sigma8.000} O_{22} (F_{1.970}Cl_{0.020})_{\Sigma1.990}$. Les paramètres réticulaires, les coordonnées de tous les atomes, et la dispersion d'électrons aux sites O3, $M1$, $M2$, $M3$, $M4$, A, et $A(m)$ ont été affinés. En accord avec l'occupation des sites fondée sur les données en diffraction X sur poudres et les données de Mössbauer, le Fe^{2+} est assigné

§   *E-mail address*: antonio.gianfagna@uniroma1.it

aux sites $M2$ et $M3$, et tout le Fe^{3+} est assigné au site $M2$. La teneur en Fe^{2+} de chaque site $M2$ dépasse largement (0.125 *apfu*) la teneur au site $M3$ (0.037 *apfu*). On peut adopter les procédures analytiques utilisées ici pour toutes sortes de fibres minérales, qu'elles soient une amphibole asbestiforme ou non. En plus de l'intérêt minéralogique, ces résultats sont pertinents dans les domaines de l'environnement et de la santé. Les interactions entre fibres minérales et le milieu biologique sont fortement liées à la chimie cristalline de ces matériaux fibreux.

(Traduit par la Rédaction)

Mots-clés: amphiboles calciques fibreuses, fluoro-édenite, spectroscopie de Mössbauer, méthode de Rietveld, micro-analyses en dispersion d'énergie, chimie cristalline, volcan Etna, Biancavilla, Italie.

Introduction

Increasing attention is being devoted to the mineralogical characterization and classification of fibrous amphiboles (not regulated as "asbestos") showing morphologies and compositions similar to those particles classified as asbestos (Wylie & Verkouteren 2000, Bandli *et al.* 2003, Meeker *et al.* 2003, Gunter *et al.* 2003). The overall aim of these investigations is to obtain a large amount of quantitative analytical data in order to better and unequivocally describe these amphiboles, because environmental exposure to mineral fibers not classified as asbestos is becoming a health concern to the general public. In Italy, for example, there are some geographical areas affected by environmental exposures to mineral fibers from non-industrial sources, and thus conducive to pathologies not connected to occupational exposure. The recent case of Biancavilla, Italy, is known also to the international scientific community (Paoletti *et al.* 2000). This is a typical example of non-occupational exposure of environmental nature, caused by natural occurrences of the fibrous amphibole fluoro-edenite (Comba *et al.* 2003, Gianfagna *et al.* 2003). Preliminary results of toxicological studies, both *in vitro* (Cardile *et al.* 2004) and *in vivo* (Soffritti *et al.* 2004), on the prismatic and fibrous variety of this new amphibole from Biancavilla, confirmed that the prismatic morphology is less harmful than the fibrous morphology, especially when related to its widespread environmental presence. We undertook a detailed crystal-chemical study of fibrous fluoro-edenite to shed light on differences in disease potential, based on both morphology and chemistry. We are convinced that differences in fiber composition also are directly related to specific pathologies in humans. As a result, in the present work we wish to obtain unequivocal data on crystal chemistry and crystal structure of the amphibole fibers from Biancavilla. These data will be extremely useful in correlations with the anticipated biological and toxicological investigations on the same materials.

Background Information

Fluoro-edenite, a new end-member of the Ca-amphibole group (Gianfagna & Oberti 2001), has the ideal formula $[NaCa_2Mg_5(Si_7Al)_8O_{22}F_2]$. It is dispersed throughout the altered volcanic rocks that characterize the Monte Calvario locality, near Biancavilla, a small town located to the southwest of the Etna Volcanic Complex, in the province of Catania, Sicily, Italy (Fig. 1). The altered and loosely consolidated rocks are mostly represented by clasts of metasomatized autobrecciated benmoreitic lavas and, in some cases, also by pyroclastic materials (Duncan 1976, Romano 1982). A thorough and recent geological and volcanological description of the area investigated is reported in a recent paper by Burragato *et al.* (2005), in which the local environmental problems of Biancavilla are assessed. The fluoro-edenite amphibole is found in both prismatic and fibrous morphologies (Fig. 2), within the matrix, the cracks, and the pores of benmoreitic host-rocks. For the prismatic variety, a crystal-chemical characterization was easily carried out (Gianfagna & Oberti 2001), whereas for the fibrous one, several complications in sampling and consequent analytical difficulties were encountered because of the very small width of the fibers (mean width 0.4–0.5 μm; mean length 30–40 μm).

Gianfagna *et al.* (2003) reported preliminary findings concerning these thin mineral fibers, but the greatest analytical difficulty was the great heterogeneity of the material, which contains an association of fibrous amphibole with numerous other microminerals, mostly represented by K-feldspar, ortho- and clinopyroxene, fluoroapatite, and abundant Fe–Ti oxides. In the present work, we overcame this problem by adopting a specific method of separation (described in the next section), which allows a strong concentration of the fibers in the mixture.

Experimental

Sample preparation

The fibrous material used for this work comes from the Poggio Mottese locality, north–northwest of the Mount Calvario quarry area, on the outskirts of the town of Biancavilla (Fig. 1c). The sampled material represents the "autobrecciated" (crushed) benmoreitic lava (Romano 1982), occurring as loosely consolidated material of a dark gray-brown color; it also contains massive pieces of scoria and crushed lava. This material
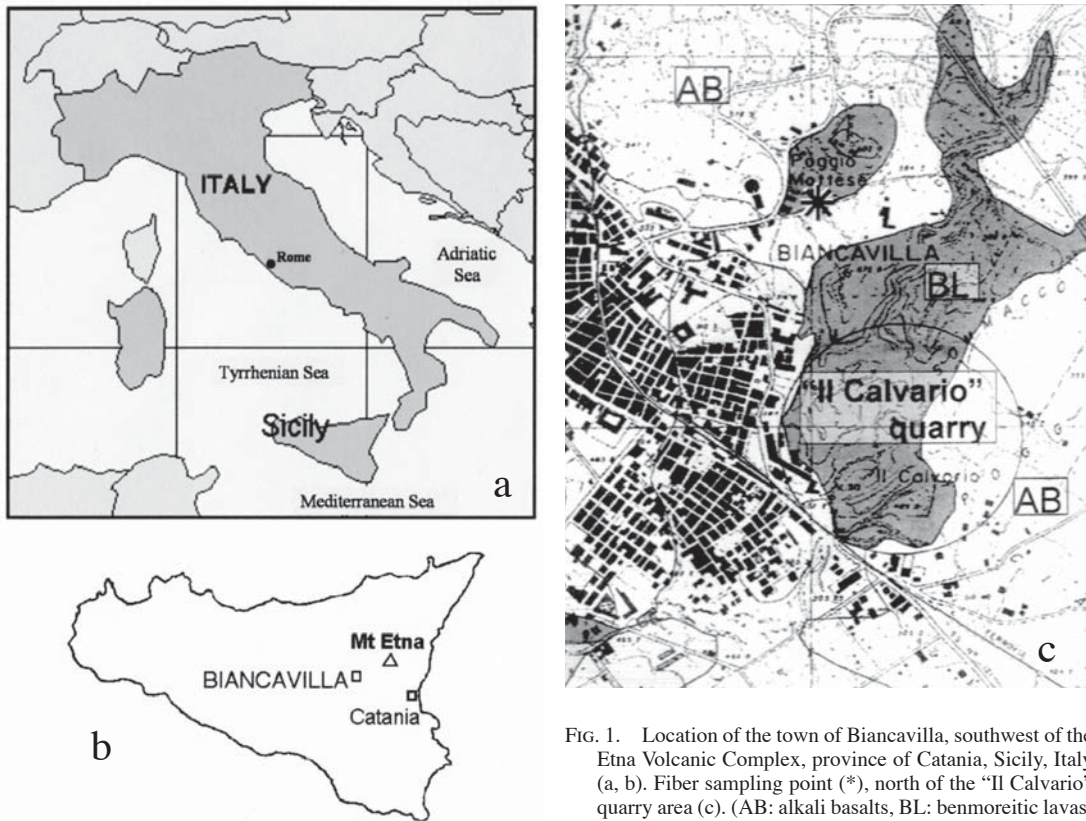
Fig. 1.   Location of the town of Biancavilla, southwest of the Etna Volcanic Complex, province of Catania, Sicily, Italy (a, b). Fiber sampling point (*), north of the "Il Calvario" quarry area (c). (AB: alkali basalts, BL: benmoreitic lavas; taken from Romano 1982).
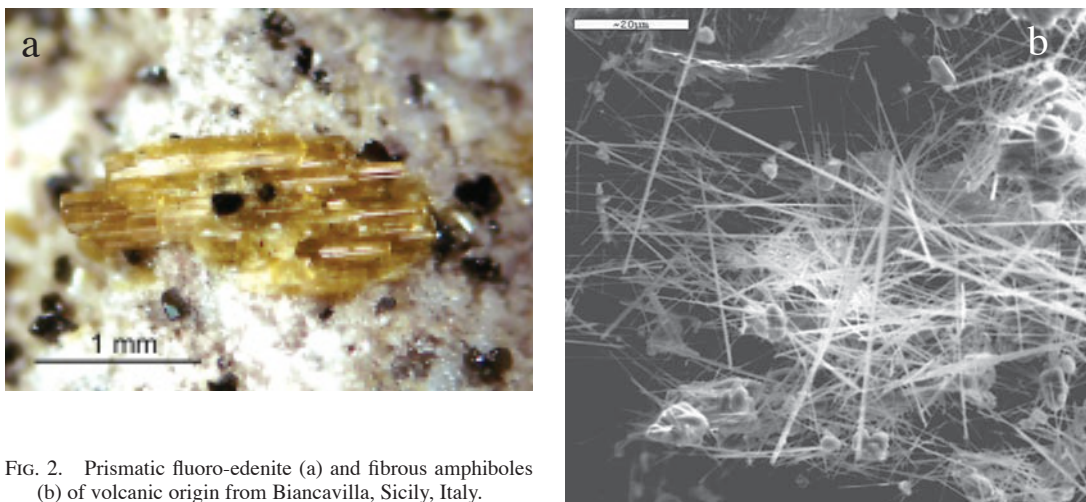

Fig. 2.   Prismatic fluoro-edenite (a) and fibrous amphiboles (b) of volcanic origin from Biancavilla, Sicily, Italy.

includes a complex mineralogical association mainly composed of microcrystals of alkali feldspar, ortho- and clinopyroxene, fluorapatite, and Fe–Ti oxides. The fibrous amphibole is abundantly present as loose fibers, not arranged in bundles, with lengths of up to 40–50 μm and a width of <1 μm (Fig. 2). A preliminary morpho- logical and mineralogical description was reported by Gianfagna *et al.* (2003); unfortunately, in that investiga- tion it was not possible to separate the fibrous fluoro- edenite from the other micro-minerals.

In the present work, we developed a method to concentrate the amphibole fibers. A simple technique of gravimetric sedimentation in water was used for the fine volcanic material from Biancavilla. We exploited both the differences in densities of the minerals and their different morphologies (*e.g.*, the strongly asymmetrical shape of the amphibole fibers).

After removing the largest fragments of rock in the original material and damp sieving the finest resulting material (<63 μm), which contained about 25% amphibole fibers, 70% feldspar, and 5% other minerals, an amount of about 200 grams of this material was dispersed with doubly-distilled water in a 5-liter transparent glass beaker. The floating material was checked by X-ray diffraction, and enrichment >95% in amphibole fibers was obtained after 30–35 hours of sedimentation. The remaining 5% is mainly composed of microgranular alkali feldspar. The opalescent floating material was filtered on a polycarbonate filter (Ø = 4.5 cm), then dried in a furnace and weighed. About 20–30 mg of the fibers was obtained after every filtra- tion, depending on the fiber content in the original material.

SEM–EDS micro-analysis

The chemical composition of the amphibole fibers was established with a micro-analytical method by using a scanning electron microscope (SEM), Zeiss DSM140A model, equipped with a Link EDS micro- analysis system. Operating conditions were: 15 kV, sample current 3.5 A, working distance 25 mm. To carry out semiquantitative analyses of the fibrous amphibole by energy-dispersion spectroscopy (EDS), and thus calculate its crystal-chemical formula, a specific analytical method was applied, which considers the composition of the prismatic fluoro-edenite as a reference material. As reported by Gianfagna & Oberti (2001), the prismatic fluoro-edenite from Biancavilla shows a certain compositional variability. As a result, electron-microprobe analyses (EMPA) were carried out on several crystals from the same locality, in order to check their composition. In Table 1, we report the chemical composition of the prismatic fluoro-edenite crystal used for SEM–EDS standardization, chosen for its dimensions (0.5 mm thickness, 1 mm length) and purity. Moreover, to avoid substantial differences in analytical conditions in the SEM–EDS, *i.e.,* sample

morphologies, as well as instrumental operating condi- tions, both the fibers and prismatic fluoro-edenite were mounted on the same sample holder (aluminum stub, Ø = 12 mm, with double adhesive carbon tape). The prismatic fluoro-edenite was first pulverized (to avoid the influence of size differences between fibers and crystals on Na, Mg, and Al determinations), and some EDS spectra were carried out to assess analytical repro- ducibility. The EDS spectrum of each fiber, obtained in the same conditions as the prismatic fluoro-edenite, was overlapped onto that of the prismatic fluoro-edenite, and the oxide ratios and percentages were calculated for every measured element (Table 2). In Tables 3, 4, and 5, we report the crystal-chemical formula of the analyzed fibers, also grouped compositionally by amphibole type (Figs. 3, 4).

57Fe Mössbauer spectroscopy

The amphibole fibers were ground gently in an agate mortar with acetone and mixed with a powdered acrylic resin to avoid (or reduce) preferred orientation. Only 10 mg of the sample was available, and total Fe content was less than 5% in weight, so that the absorber was within the limits for the thin absorber thickness described by Long *et al.* (1983). For the prismatic

TABLE 1. AVERAGE CHEMICAL COMPOSITION DERIVED FROM THREE ANALYSES[§] OF THE PRISMATIC FLUORO-EDENITE CRYSTAL USED AS A REFERENCE MATERIAL TO ANALYZE THE FIBROUS AMPHIBOLES FROM BIANCAVILLA

Oxides	wt%	est. σ	Sites	*apfu*	est. σ
SiO_2	52.83	0.01	Si	7.327	0.013
TiO_2	0.55	0.01	^{IV}Al	0.623	0.005
Al_2O_3	3.81	0.04	ΣT	7.950	
FeO_{tot}	2.25	0.11			
MnO	0.46	0.04	^{VI}Al	0.000	0.000
MgO	23.60	0.06	Fe^{3+}	0.239	0.012
CaO	10.73	0.29	Fe^{2+}	0.022	0.001
Na_2O	3.04	0.01	Mg	4.628	0.017
K_2O	0.82	0.02	Ti	0.057	0.001
F	4.11	0.22	Mn	0.054	0.005
Cl	0.05	0.03	ΣC	5.000	
F, Cl =O	1.74	0.10			
			Mg	0.251	0.016
Total	100.51	0.75	Ca	1.594	0.043
			Na	0.154	0.037
* Fe_2O_3	2.29		ΣB	2.000	
* FeO	0.19				
			Na	0.663	0.034
			K	0.146	0.004
			ΣA	0.809	0.031
			F	1.803	0.094
			Cl	0.011	0.008
			$\Sigma O3$	1.814	
			^BNa	0.154	0.037
			$^A(Na + K)$	0.809	0.031

[§] Analyzed with an electron microprobe. * Fe^{3+}/Fe_{tot} = 0.916, by Mössbauer spectroscopy. The allotment of ions to the various sites is made on the basis of 24 (O + F + Cl) atoms per formula unit (*apfu*).

TABLE 2. RESULTS OF QUANTITATIVE SEM–EDS MICRO-ANALYSES
OF THE FIBROUS AMPHIBOLE FROM BIANCAVILLA

	1	2	3	4	5	6	7	8	9	10	11	12	13
SiO_2 wt%	54.03	53.91	53.25	52.24	53.84	55.33	52.19	52.14	51.89	53.47	54.70	53.65	53.85
TiO_2	0.70	0.57	0.56	0.48	0.74	0.48	0.60	0.85	0.51	0.42	0.70	0.54	0.67
Al_2O_3	4.17	3.43	3.29	3.62	3.57	3.38	3.33	3.58	3.49	2.57	3.09	4.04	3.39
FeO_{tot}	3.70	4.67	5.22	4.36	4.07	4.08	4.25	4.66	4.13	5.72	3.71	4.45	4.34
MnO	0.75	0.48	0.47	0.89	0.52	0.50	0.35	0.48	0.43	0.58	0.34	0.46	0.49
MgO	19.42	19.24	18.28	21.90	20.57	20.08	22.96	22.03	22.67	20.61	21.14	18.62	19.54
CaO	9.56	10.68	11.47	10.41	10.58	9.46	9.74	9.74	10.26	10.19	10.09	11.80	10.84
Na_2O	3.67	3.15	3.67	2.44	2.48	3.02	2.94	2.90	2.89	2.89	2.55	2.75	2.94
K_2O	1.08	0.99	0.84	0.87	0.74	0.75	0.77	0.74	0.84	0.68	0.81	0.81	1.05
F [†]	4.46	4.46	4.46	4.46	4.46	4.46	4.46	4.46	4.46	4.46	4.46	4.46	4.46
Cl	0.11	0.08	0.12	0.07	0.07	0.10	0.06	0.07	0.08	0.07	0.07	0.08	0.08
F,Cl=O	1.90	1.90	1.91	1.89	1.89	1.90	1.89	1.89	1.90	1.89	1.89	1.90	1.90
Total	99.75	99.76	99.75	99.85	99.75	99.74	99.76	99.76	99.75	99.77	99.76	99.77	99.75
* Fe_2O_3	2.76	3.49	3.90	3.26	3.04	3.05	3.18	3.48	3.09	4.27	2.77	3.32	3.24
* FeO	1.21	1.53	1.71	1.43	1.34	1.34	1.39	1.53	1.36	1.88	1.22	1.46	1.42

	14	15	16	17	18	19	20	21	22	23	24	25
SiO_2 wt%	53.79	53.11	55.64	53.20	55.78	52.28	52.81	56.67	53.22	54.36	56.84	54.00
TiO_2	0.53	0.68	0.37	0.64	0.43	0.53	0.55	0.66	0.67	0.88	0.68	0.39
Al_2O_3	3.05	4.64	3.48	3.26	3.71	3.94	3.99	3.23	3.71	3.44	3.55	3.82
FeO_{tot}	3.03	3.20	4.34	4.74	4.66	4.34	4.09	3.51	5.85	3.87	3.42	3.80
MnO	0.33	0.40	0.86	0.43	0.57	0.37	0.77	0.57	0.55	0.63	0.58	0.49
MgO	23.49	21.65	20.14	20.69	18.93	21.76	20.29	19.51	19.41	20.57	17.22	20.32
CaO	9.41	9.73	8.41	10.40	9.23	10.33	10.81	8.64	9.60	9.09	10.54	10.36
Na_2O	2.71	2.82	2.74	3.07	2.79	2.70	2.85	3.39	3.19	3.21	3.14	3.08
K_2O	0.78	0.87	1.12	0.65	1.00	0.87	0.93	0.93	0.90	1.03	1.13	0.86
F [†]	4.46	4.46	4.46	4.46	4.46	4.46	4.46	4.46	4.46	4.46	4.46	4.46
Cl	0.06	0.09	0.11	0.10	0.10	0.07	0.10	0.09	0.08	0.11	0.09	0.07
F,Cl=O	1.89	1.90	1.90	1.90	1.90	1.89	1.90	1.90	1.90	1.90	1.90	1.89
Total	99.75	99.75	99.77	99.74	99.76	99.76	99.76	99.76	99.75	99.76	99.75	99.77
* Fe_2O_3	2.26	2.39	3.24	3.54	3.48	3.24	3.06	2.62	4.37	2.89	2.55	2.84
* FeO	0.99	1.05	1.42	1.55	1.53	1.42	1.34	1.15	1.92	1.27	1.12	1.25

* $Fe^{3+}/Fe_{tot} = 0.672$, by Mössbauer spectroscopy. [†] The value indicated is the maximum content of F in an anhydrous amphibole.

fluoro-edenite, a second absorber was prepared with the same precautions, but in this case 25 mg of the sample had to be hand-picked because its total Fe content is less than 2% in weight. The spectra were collected at room temperature (RT) using a conventional spectrometer system operated in constant acceleration mode with a ^{57}Co source of nominal strength of 50 mCi in a rhodium matrix. The spectral data were recorded in a multichannel analyzer using 512 channels for both the velocity ranges –4 to 4 mm/s and –8 to 8 mm/s. To obtain good counting-statistics, the data-collection time varied from two to four weeks. After velocity calibration against a spectrum of high-purity α-iron foil (25 μm thick), the raw data were folded to 256 channels. The spectra were fitted using the Recoil 1.04 fitting program (Lagarec & Rancourt 1988). A first cycle was performed by fitting pure Lorentzian line-shapes (as used by most investigators). For the prismatic fluoro-edenite, a good
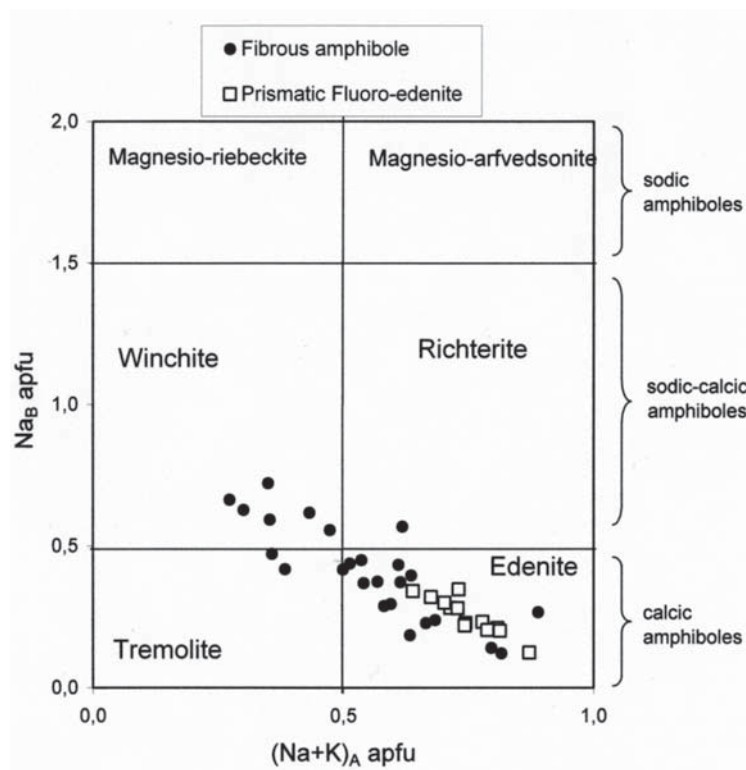
FIG. 3. Two-dimensional classification graph [(Na+K)$_A$ versus Na$_B$] in which are plotted the compositions of the fibrous amphiboles, compared with the prismatic fluoro-edenite from Biancavilla. Modified after Leake et al. (1997).
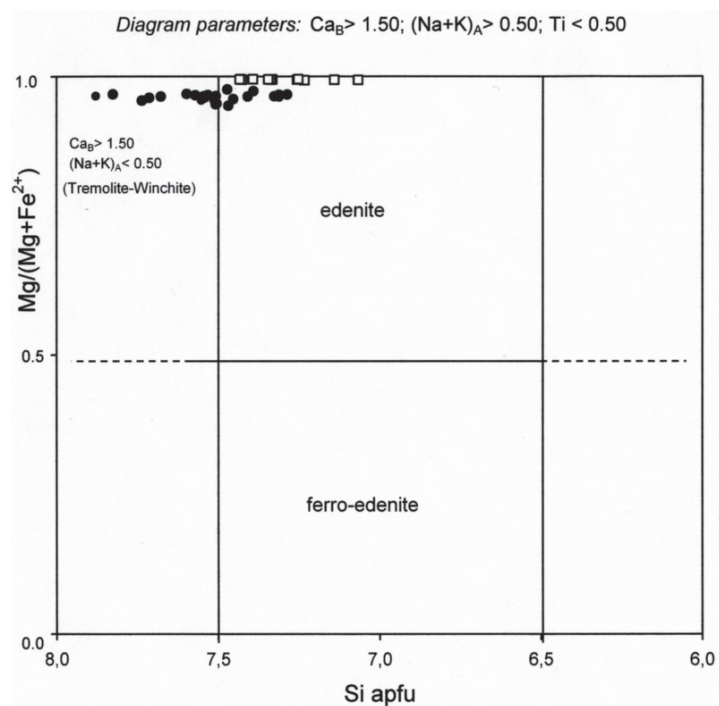

FIG. 4. Classification of the calcic amphiboles on the basis of the Si content (apfu) versus Mg/(Mg + Fe^{2+}) ratio. Modified after Leake et al. (1997).

TABLE 3. CRYSTAL-CHEMICAL FORMULAE OF THE 25 SAMPLES OF FIBROUS AMPHIBOLE OF TABLE 2, CALCULATED ON THE BASIS OF 24 *apfu* (O + F + Cl)

	2	3	4	7	8	9	10	12	13	14	17	19	20
T site													
Si	7.553	7.509	7.329	7.311	7.311	7.286	7.505	7.515	7.542	7.472	7.454	7.326	7.409
^{IV}Al	0.447	0.491	0.598	0.550	0.591	0.577	0.424	0.485	0.458	0.500	0.538	0.651	0.591
Σ*T*	8.000	8.000	7.927	7.861	7.902	7.863	7.929	8.000	8.000	7.972	7.992	7.977	8.000
C site													
^{VI}Al	0.119	0.056	0.000	0.000	0.000	0.000	0.000	0.183	0.102	0.000	0.000	0.000	0.069
Fe^{3+}	0.368	0.414	0.344	0.335	0.367	0.326	0.451	0.350	0.342	0.237	0.373	0.342	0.323
Fe^{2+}	0.179	0.202	0.168	0.163	0.179	0.159	0.220	0.171	0.167	0.115	0.182	0.167	0.157
Mg	4.020	3.842	4.331	4.397	4.307	4.411	4.215	3.888	4.080	4.555	4.320	4.393	4.244
Ti	0.060	0.060	0.051	0.064	0.090	0.053	0.044	0.057	0.071	0.055	0.068	0.055	0.059
Mn	0.057	0.057	0.106	0.041	0.056	0.051	0.069	0.054	0.058	0.038	0.051	0.044	0.092
Σ*C*	4.803	4.631	5.000	5.000	5.000	5.000	5.000	4.703	4.819	5.000	4.994	5.000	4.943
B site													
Mg	0.000	0.000	0.249	0.397	0.298	0.334	0.097	0.000	0.000	0.310	0.000	0.152	0.000
Ca	1.604	1.733	1.566	1.462	1.463	1.544	1.534	1.772	1.627	1.402	1.562	1.552	1.625
Na	0.396	0.267	0.185	0.141	0.239	0.122	0.369	0.228	0.373	0.288	0.438	0.296	0.375
Σ*B*	2.000	2.000	2.000	2.000	2.000	2.000	2.000	2.000	2.000	2.000	2.000	2.000	2.000
A site													
Na	0.458	0.737	0.478	0.658	0.550	0.665	0.418	0.520	0.426	0.443	0.396	0.439	0.402
K	0.177	0.152	0.155	0.138	0.133	0.151	0.122	0.145	0.188	0.139	0.117	0.156	0.166
Σ*A*	0.635	0.889	0.633	0.796	0.683	0.816	0.540	0.665	0.614	0.582	0.513	0.595	0.568
O3 site													
F	1.975	1.988	1.978	1.975	1.977	1.980	1.978	1.975	1.975	1.959	1.975	1.976	1.978
Cl	0.020	0.030	0.017	0.014	0.016	0.018	0.016	0.019	0.019	0.014	0.024	0.016	0.024
ΣO3	1.995	2.018	1.995	1.989	1.993	1.998	1.996	1.994	1.994	1.973	1.999	1.992	2.002
^{B}Na	0.396	0.267	0.186	0.141	0.239	0.122	0.369	0.228	0.373	0.288	0.438	0.296	0.375
^{A}(Na + K)	0.635	0.889	0.633	0.796	0.683	0.816	0.540	0.665	0.614	0.582	0.513	0.595	0.568
Si	7.553	7.509	7.329	7.311	7.311	7.286	7.505	7.515	7.542	7.472	7.454	7.326	7.409
Mg#	0.957	0.950	0.965	0.967	0.963	0.968	0.951	0.958	0.961	0.977	0.960	0.965	0.964

	24	25	6	16	18	21	22	23	5	11	15	1
T site												
Si	7.878	7.533	7.678	7.714	7.736	7.826	7.469	7.572	7.508	7.598	7.391	7.546
^{IV}Al	0.122	0.467	0.322	0.286	0.264	0.174	0.531	0.428	0.492	0.402	0.609	0.454
Σ*T*	8.000	8.000	8.000	8.000	8.000	8.000	8.000	8.000	8.000	8.000	8.000	8.000
C site												
^{VI}Al	0.458	0.162	0.231	0.282	0.342	0.351	0.082	0.136	0.096	0.105	0.151	0.232
Fe^{3+}	0.266	0.298	0.318	0.338	0.363	0.272	0.461	0.303	0.319	0.289	0.250	0.290
Fe^{2+}	0.130	0.146	0.155	0.165	0.177	0.133	0.225	0.148	0.156	0.141	0.122	0.142
Mg	3.558	4.225	4.154	4.076	3.915	4.016	4.060	4.246	4.276	4.352	4.359	4.042
Ti	0.071	0.041	0.050	0.038	0.044	0.069	0.071	0.092	0.078	0.073	0.072	0.074
Mn	0.069	0.057	0.058	0.101	0.068	0.067	0.066	0.075	0.061	0.040	0.047	0.089
Σ*C*	4.552	4.929	4.967	5.000	4.909	4.908	4.966	5.000	4.986	5.000	5.000	4.870
B site												
Mg	0.000	0.000	0.000	0.087	0.000	0.000	0.000	0.025	0.000	0.026	0.132	0.000
Ca	1.566	1.549	1.407	1.250	1.373	1.279	1.444	1.358	1.582	1.502	1.451	1.431
Na	0.434	0.451	0.593	0.663	0.627	0.721	0.556	0.617	0.418	0.472	0.417	0.569
Σ*B*	2.000	2.000	2.000	2.000	2.000	2.000	2.000	2.000	2.000	2.000	2.000	2.000
A site												
Na	0.410	0.383	0.220	0.075	0.124	0.186	0.312	0.249	0.251	0.214	0.345	0.426
K	0.200	0.153	0.133	0.198	0.177	0.164	0.161	0.183	0.132	0.144	0.155	0.192
Σ*A*	0.610	0.536	0.353	0.273	0.301	0.350	0.473	0.432	0.383	0.358	0.500	0.618
O3 site												
F	1.954	1.967	1.957	1.954	1.956	1.947	1.979	1.964	1.967	1.959	1.962	1.969
Cl	0.021	0.016	0.023	0.026	0.023	0.021	0.019	0.026	0.016	0.016	0.021	0.026
ΣO3	1.975	1.983	1.980	1.980	1.979	1.968	1.998	1.990	1.983	1.975	1.983	1.995
^{B}Na	0.434	0.451	0.593	0.663	0.627	0.721	0.556	0.617	0.418	0.472	0.417	0.569
^{A}(Na + K)	0.610	0.536	0.353	0.273	0.301	0.350	0.473	0.432	0.384	0.358	0.499	0.618
Si	7.878	7.533	7.678	7.714	7.736	7.826	7.469	7.572	7.508	7.598	7.391	7.546
Mg#	0.965	0.967	0.964	0.962	0.957	0.968	0.947	0.967	0.965	0.969	0.974	0.966

The formulae are grouped according to variable contents of ^{A}(Na + K) *versus* ^{B}Na, and Si *versus* Mg/(Mg + Fe^{2+}); see Figures 3 and 4, respectively). Columns 2, 3, 4, 7, 8, 9, 10, 12, 13, 14, 17, 19, 20, 24 and 25: fluoro-edenite; columns 6, 16, 18, 21, 22 and 23: F analog of winchite; columns 5, 11 and 15: F analog of tremolite; column 1: fluororichterite. Mg#: Mg / (Mg + Fe^{2+}).

fit was obtained (reasonable parameters and $\chi^2 = 1.46$) with four doublets ($1Fe^{2+} + 3Fe^{3+}$), but for the fibers, the results obtained were not satisfactory because of the extremely wide line-widths (up to 2 mm/s). In fact, it has been shown that the pure Lorentzian approach fails when analyzing spectra with poorly resolved quadrupole doublets (Rancourt & Ping 1991, Rancourt 1994a). Accordingly, a second cycle of refinement was carried out by fitting quadrupole-splitting distributions (QSD), following the successful approach of Gunter *et al.* (2003). A number of fitting models with unconstrained parameters [isomer shift (δ_0), coupling parameter (δ_1), center of a Gaussian component (Δ_0), Gaussian width (σ_Δ), and absorption area (A)] were tried in order to obtain the best fit. A model based on two sites ($1Fe^{2+} + 1Fe^{3+}$) each with two components was finally chosen ($\chi^2 = 0.58$), as increasing the number of Gaussian components did not change the resulting distribution significantly. This gave us confidence in the physical correctness of both the coupling parameters (0.027 or less) and the distribution analysis. Uncertainties were calculated using the covariance matrix, and errors were estimated to be no less than ±3% for both Fe^{2+} and Fe^{3+} absorption areas (Table 6, Fig. 5).

XRD analysis

The powder-diffraction data were collected on a Siemens D5005 fully automated parallel-beam diffractometer operating in transmission mode, equipped with a solid-state Peltier-cooled Si(Li) detector. The fibers were ground in ethanol in an agate mortar. After evaporation, the powder was charged in a 0.3 mm diameter borosilicate glass capillary. A reasonable compaction was obtained *via* an ultrasonic cleaner. The capillary was mounted and aligned on a standard goniometer head and fixed to the sample holder of the diffractometer. Preliminary observation of the diffraction pattern indicated the presence of minor albite that was therefore included in the Rietveld refinement. The data were evaluated by the GSAS suite of crystallographic programs (Larson & Von Dreele 1985) using the EXPGUI graphical user interface (Toby 2001). The background was fitted with a 36-term Chebyshev polynomial in order to properly model the contribution from amorphous material arising from the capillary. The peak shape was modeled by the TCH pseudo-Voigt function (Thompson *et al.* 1987) modified for asymmetry (Finger *et al.* 1994). The refined variables were GV and GW (tanθ-dependent and angle-independent, respectively) Gaussian parameters, LY (tanθ-dependent) Lorentzian, and S/L and H/L asymmetry parameters (constrained to be equal in magnitude). Refinement of two independent scale-factors for amphibole and albite allowed a quantitative analysis of the mixture. The starting structural parameters of the fibers were those of prismatic fluoro-edenite of Gianfagna & Oberti (2001), whereas those of Meneghinello *et al.* (1999) were selected for the albite. The isotropic displacement parameters were kept fixed throughout the refinement to the values refined for prismatic fluoro-edenite (Gianfagna & Oberti 2001). The geometry of the system was partly constrained under the following conditions: ^{IV}T–O $\times$ 8 = 1.635(25) Å, O–O $\times$ 12 = 2.67(4) Å, $^{VI}M1$–O = 2.06(2) Å, $^{VI}M2$–O = 2.08(3) Å, $^{VI}M3$–O = 2.05(2) Å, $^{VIII}M4$–O = 2.51(20)

TABLE 4. CRYSTAL-CHEMICAL FORMULAE OF FOUR REPRESENTATIVE TYPES OF FIBROUS AMPHIBOLE ANALYZED*

#	Type of amphibole	Crystal-chemical formula§
15	Edenite	$(Na_{0.370}K_{0.153})_{\Sigma0.523}(Ca_{1.571}Na_{0.429})_{\Sigma2.000}$ $(^{VI}Al_{0.038}Fe^{3+}_{0.342}Fe^{2+}_{0.167}Mg_{4.308}Ti_{0.060}Mn_{0.060})_{\Sigma4.975}$ $(Si_{7.462}{}^{IV}Al_{0.538})_{\Sigma8.000}O_{22}(F_{1.975}Cl_{0.019})_{\Sigma1.994}$
6	Winchite	$(Na_{0.195}K_{0.169})_{\Sigma0.364}(Ca_{1.352}Na_{0.819}Mg_{0.819})_{\Sigma2.000}$ $(^{VI}Al_{0.237}Fe^{3+}_{0.343}Fe^{2+}_{0.167}Mg_{4.078}Ti_{0.061}Mn_{0.072})_{\Sigma4.958}$ $(Si_{7.666}{}^{IV}Al_{0.334})_{\Sigma8.000}O_{22}(F_{1.959}Cl_{0.023})_{\Sigma1.982}$
3	Tremolite	$(Na_{0.270}K_{0.144})_{\Sigma0.414}(Ca_{1.511}Na_{0.436}Mg_{0.053})_{\Sigma2.000}$ $(^{VI}Al_{0.117}Fe^{3+}_{0.286}Fe^{2+}_{0.149}Mg_{4.329}Ti_{0.074}Mn_{0.049})_{\Sigma4.995}$ $(Si_{7.499}{}^{IV}Al_{0.501})_{\Sigma8.000}O_{22}(F_{1.982}Cl_{0.018})_{\Sigma1.980}$
1	Richterite	$(Na_{0.426}K_{0.192})_{\Sigma0.618}(Ca_{1.431}Na_{1.569})_{\Sigma2.000}$ $(^{VI}Al_{0.232}Fe^{3+}_{0.290}Fe^{2+}_{0.142}Mg_{4.042}Ti_{0.074}Mn_{0.089})_{\Sigma4.869}$ $(Si_{7.546}{}^{IV}Al_{0.454})_{\Sigma8.000}O_{22}(F_{1.969}Cl_{0.025})_{\Sigma1.994}$

* See Table 3. #: number of analyses made. § On the basis of 24 = O + F + Cl atoms per formula unit (*apfu*).

TABLE 5. AVERAGE CHEMICAL COMPOSITION DERIVED FROM 25 ANALYSES§ OF THE FIBROUS AMPHIBOLE FROM BIANCAVILLA, WITH MINIMUM–MAXIMUM VARIATIONS

Oxides	wt%	est. σ	Range	Sites	*apfu*	Range
SiO_2	53.85	1.34	51.89 - 56.84	Si	7.520	7.286 - 7.878
TiO_2	0.59	0.13	0.37 - 0.88	^{IV}Al	0.480	0.122 - 0.651
Al_2O_3	3.55	0.41	2.57 - 4.64	ΣT	8.000	7.861 - 8.000
FeO_{tot}	4.25	0.67	3.03 - 5.85			
MnO	0.53	0.15	0.33 - 0.89	^{VI}Al	0.104	0.000 - 0.458
MgO	20.44	1.49	17.22 - 23.49	Fe^{3+}	0.333	0.237 - 0.461
CaO	10.06	0.79	8.41 - 11.80	Fe^{2+}	0.162	0.115 - 0.225
Na_2O	2.96	0.31	2.44 - 3.67	Mg	4.255	3.558 - 4.555
K_2O	0.88	0.13	0.65 - 1.13	Ti	0.062	0.038 - 0.092
F	4.46	0.00	4.46 - 4.46	Mn	0.063	0.038 - 0.106
Cl	0.08	0.02	0.06 - 0.12	ΣC	4.980	4.552 - 5.000
F, Cl =O	1.90					
				Mg	0.000	0.000 - 0.397
Total	99.76			Ca	1.505	1.250 - 1.772
				Na	0.495	0.122 - 0.721
* Fe_2O_3	3.17		2.26 - 4.37	ΣB	2.000	2.000
* FeO	1.39		0.99 - 1.92			
				Na	0.307	0.075 - 0.737
				K	0.157	0.117 - 0.200
				ΣA	0.464	0.273 - 0.889
				F	1.970	1.947 - 1.988
				Cl	0.020	0.014 - 0.030
				$\Sigma O3$	1.990	1.968 - 2.018
				^BNa	0.495	0.122 - 0.721
				$^A(Na+K)$	0.464	0.273 - 0.889

§ Analyzed with SEM–EDS. * $Fe^{3+}/Fe_{tot} = 0.672$, by Mössbauer spectroscopy. The allotment of ions to the various sites is made on the basis of 24 (O + F + Cl) atoms per formula unit (*apfu*).

TABLE 6. ^{57}Fe MÖSSBAUER HYPERFINE PARAMETERS FOR PRISMATIC
AND FIBROUS FLUORO-EDENITE AT ROOM TEMPERATURE

Lineshape	χ^2	Fe^{2+}				Fe^{3+}				Fe^{3+}_{raw} % Fe_{tot}	Fe^{3+}_{corr} % Fe_{tot}
		Δ_0 mm/s	σ_Δ mm/s	δ_0 mm/s	Area %	Δ_0 mm/s	σ_Δ mm/s	δ_0 mm/s	Area %		
Prismatic											
Lorentzian	1.46	1.47		0.99	7.3	0.39		0.28	25.6	92.7	91.6
						0.95		0.33	43.3		
						1.67		0.27	20.8		
Fibrous											
Lorentzian	0.64	1.88		1.13	20.3	0.80		0.39	26.2	70.6	66.3
		2.64		1.14	9.1	0.00		0.38	44.4		
QSD	0.58	1.87	0.28	1.09	18.9	0.77	0.41	0.38	31.4	71.4	67.2
		2.65	0.25	1.09	9.7	1.50	1.80	0.38	40.0		

Notes: Isomer shift (δ_0) with respect to α-iron. For the Quadrupole Splitting Distribution (QSD): $\delta_1 = 0.01$ and 0.03 for Fe^{3+} and Fe^{2+}, respectively; $\gamma = 0.194$ mm/s; $h_+/h_- = 1$. Symbols according to Rancourt & Ping (1991). Fe^{3+}_{raw} is obtained from the area of absorption peaks assigned to ferric iron. Fe^{3+}_{corr} is obtained from the previous value by applying the correction factor C = 1.22 (Dyar *et al.* 1993). Estimated uncertainties are about 0.02 mm/s for hyperfine parameters, and no less than 3% for absorption areas.
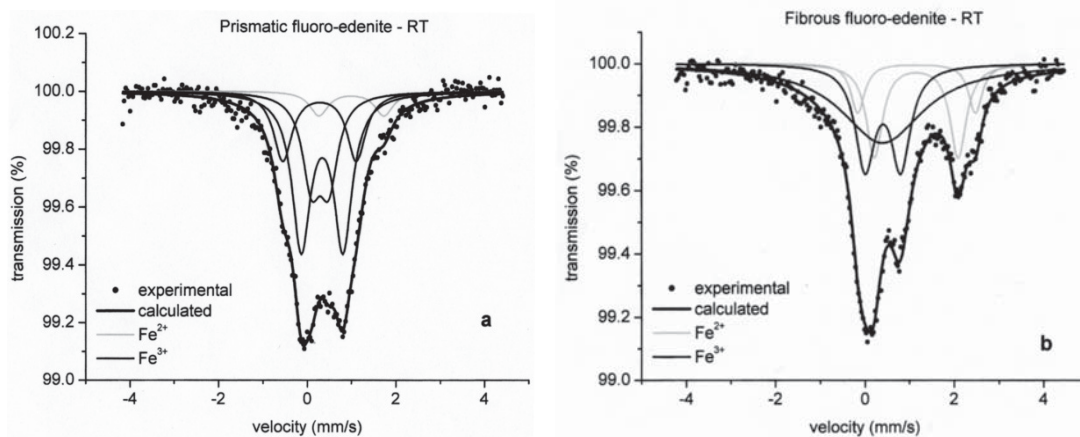

FIG. 5. Room-temperature ^{57}Fe Mössbauer spectra for prismatic (a) and fibrous fluoro-edenite (b) from Biancavilla.

Å. The weight associated with those observations was kept equal to 2 during the refinement. Because of correlation, it was not possible, despite several attempts, to independently refine the position and site scattering (s.s.) of the two adjacent A and A2 sites. Therefore, a single site A (special position: 0, 1/2, 0) was considered during the refinement. Correlation may be the reason for the reported reversed site-scattering at the A sites of prismatic fluoro-edenite between single-crystal and powder data, despite the same refined total site-scattering (*cf.* Gianfagna & Oberti 2001, Gianfagna *et al.* 2003). Cell parameters, positional parameters for all the atoms, and site scattering for O3, *M*1, *M*2, *M*3, *M*4, *A* and *A*(*m*) were refined for the fibers. Only the cell parameters were refined for the albite. Attempts to model the presence of preferred orientation by means of the generalized spherical harmonics description of Von Dreele (1997) produced only a very marginal improve-

ment of the fit as a result of a J texture index of 1.036. Convergence was reached at Rp = 5.14%, Rwp = 6.78%, RF = 4.43%, reduced χ^2 = 1.171, contribution of the restraints to χ^2 = 73.5, DWd = 1.760. The experimental details and miscellaneous data of the refinement are reported in Table 7, cell parameters and site-scattering values in Table 8, fractional coordinates and isotropic thermal parameters in Table 9, selected bond-distances in Table 10, and experimental, calculated and difference plots are displayed in Figure 6.

RESULTS AND DISCUSSION

The chemical composition measured on 25 fibers is reported in Table 2. A fixed value of 4.5 wt.% F was imposed for the fluorine content because: a) F content is difficult to assess with this method (its line partially overlaps that of oxygen); b) the OH$^-$ content is absent in both prismatic and fibrous fluoro-edenite, as verified through FTIR investigations (Gianfagna & Oberti 2001, for the prismatic variety; unpublished data for the fibers); c) an experimental F content higher than 4

wt.% was verified for prismatic fluoro-edenite analyzed by EMPA (Table 1, this work); finally, d) an average value of 4.5 wt.% F was reported by Gianfagna & Oberti (2001), and this value also represents the maximum F content of an anhydrous amphibole.

The chemical results obtained for the Biancavilla fibers show some compositional differences with respect to prismatic fluoro-edenite, in particular concerning the Mg and Ca contents (higher in the prismatic variety), and for Si and Fe (higher in the fibers). On the basis of the amphibole classification by Leake *et al.* (1997), Figure 3 shows the relationships of the compositional area relative to the fibers compared to that of the prismatic fluoro-edenite. The area for the fibers is far larger than that for the prismatic fragments, both extending around the 1:1 line and tending toward the winchite field. In Table 3, the fibers are grouped and classified on the basis of their distribution in the compositional graph of Figure 3. Four different amphiboles are present (edenite, winchite, tremolite, and richterite), and their representative crystal-chemical formulae are reported in Table 4. Fluoro-edenite is the most represented
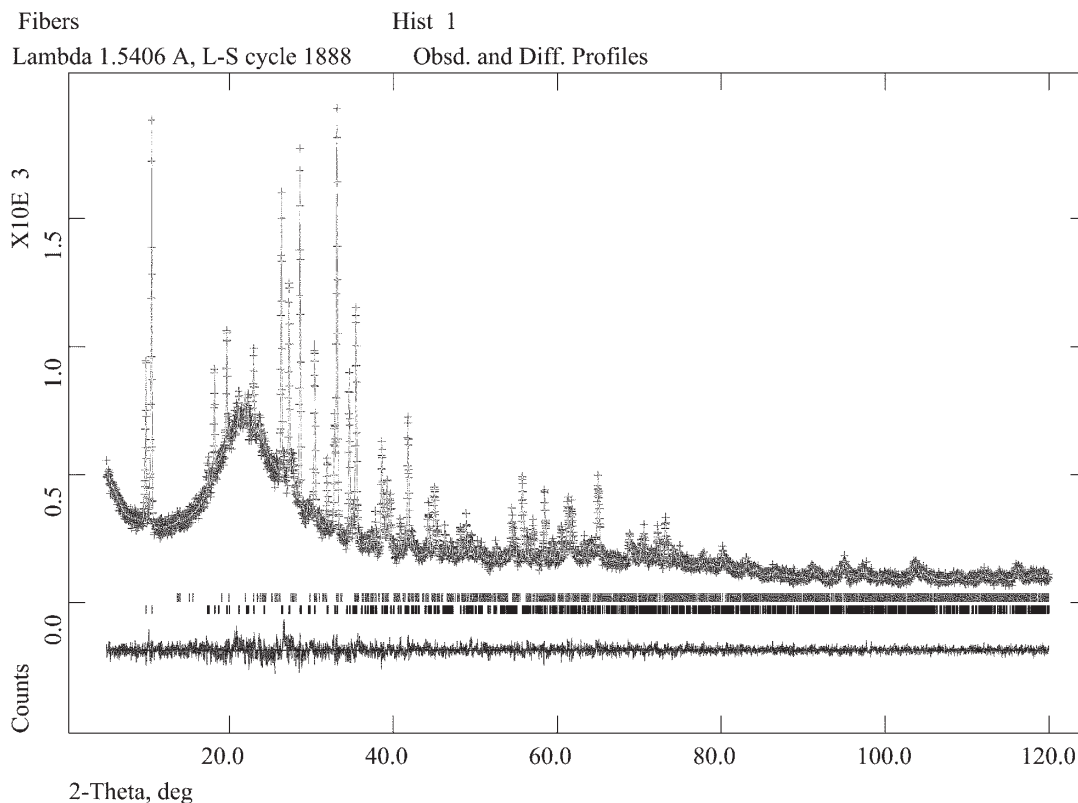

FIG. 6. Experimental (dots) and calculated (continuous line) Rietveld plots for the fibrous fluoro-edenite from Biancavilla. The difference profile is shown at the bottom of the figure. Vertical markers refer to the positions of the calculated Bragg reflections for amphibole (below) and albite (above).

(15 analyses out of 25), whereas the other types are only subordinately represented (6, 3, and 1 analyses, respectively, as seen in Table 3). Moreover, the graph of Figure 4 highlights the higher Fe content of the fibers respect to the prismatic fluoro-edenite, and also shows the compositional trend of the fibers toward the left side of the graph, that, according to Leake *et al.* (1997), is still not well defined.

The Mössbauer absorption spectrum of prismatic fluoro-edenite is composed of four quadrupole doublets, three with isomer shift values about 0.30 mm/s, and quadrupole splitting values from 0.39 to 1.67 mm/s, which were assigned to Fe^{3+}, and the fourth with an isomer shift of 0.99 mm/s and quadrupole splitting of 1.46 mm/s, which was assigned to Fe^{2+} (Fig. 5a). Note that Fe^{3+} is largely dominant over Fe^{2+} (Table 6), its proportion being 92.7% Fe_{tot} when quantified by the direct measurement of the absorption areas (Fe^{3+}_{raw}), and 91.6% when adjusting for the recoil-free fraction (Fe^{3+}_{corr}), as suggested by Dyar *et al.* (1993). The Fe^{3+}/Fe_{tot} ratio is definitely higher than that estimated in the first crystal-chemical study of fluoro-edenite from Biancavilla by Gianfagna & Oberti (2001), in which, however, no direct measurements of this ratio were available; it was recalculated on the basis of chemical and structural data.

The absorption spectrum of fibrous fluoro-edenite is typical of a paramagnetic material, and is composed of two kinds of contributions (Fig. 5b). The first one is due to Fe^{2+} components with δ_0 of about 1.1 mm/s (both in Lorentzian and QSD fits) and a roughly bimodal distribution of quadrupole splitting centered around Δ_0 of 1.87 and 2.65 mm/s in both fits. According to

specific literature for sodic–calcic amphiboles (Gunter *et al.* 2003), these components should be assigned to $^{[M2]}Fe^{2+}$ and $^{[M3]}Fe^{2+}$, respectively. However, according to Schmidbauer *et al.* (2000) and Goldman (1979), these two components should be assigned to $M4$ and ($M1 + M3$), respectively. In agreement with our XRPD data (Table 4), Fe^{2+} was assigned to the $M2$ and $M3$ sites. The second absorption contribution, as modeled by QSD, is due to Fe^{3+} components with δ_0 of 0.38 mm/s and a quadrupole-splitting distribution that is sharp at Δ_0 of 0.77 mm/s and very broad at Δ_0 of 1.50 mm/s. Similarly to what was found by Gunter *et al.* (2003), the sharp component may easily be assigned to octahedrally coordinated Fe^{3+}, but the broad one is suspect because it may derive either from the presence of oxide impurities or from local disorder around the Fe atoms, as is commonly observed in complex silicates (Andreozzi *et al.* 2004) . In our case, the first hypothesis may be excluded on the basis of both chemical and XRPD analysis. The absence of oxide impurities was further confirmed by Mössbauer investigation in the region from –10 to 10 mm/s, which shows no evidence of magnetic sextets due to Fe oxides or hydroxides. On these bases, both the sharp and the wide components were considered when quantifying the actual Fe^{3+} content (Fe^{3+}_{corr}) of our fibrous fluoro-edenite, which turned out to be 67.2% Fe_{tot} (Table 6). Notably, the Fe^{3+} contents obtained by QSD analysis are closely comparable with those retrieved by Lorentzian site analysis, the latter being underestimated by about 1%, as predicted by Rancourt (1994a, b). For our samples, all the Fe^{3+} was assigned to the $M2$ site, in agreement with the cation site-partition based on XRPD data (Table 8).

The cell parameters of the fibrous fluoro-edenite are consistent with those previously reported by Gianfagna *et al.* (2003), apart from a small increase of the b parameter [18.0188(6) Å with respect to 17.992(3) Å of the reference data]. The structure is quite similar to that of prismatic fluoro-edenite as reported by Gianfagna & Oberti (2001) from a single crystal of the same locality. The <T–O> bond distance is 1.633 Å, slightly smaller than the 1.635 Å of prismatic fluoro-edenite. In particular, the reduction is preferentially at $T1$, where Al ordering is expected to occur (Oberti *et al.* 1992). This shrinkage is consistent with the reduced Al content of the T site of the fibers (*ca.* 0.48 with respect to *ca.* 0.58 atoms per formula unit (*apfu*) of prismatic fluoro-edenite). The <$M1$–O> distance is identical (2.059 Å), but shows a larger dispersion in the case of the fibers (0.018 Å with respect to 0.002 Å). Both the <$M2$–O> and <$M3$–O> distances are only slightly larger in the case of the fibers compared the single crystal (2.085 *versus* 2.079 Å, and 2.060 *versus* 2.046 Å, respectively). The C sites ($M1 + M2 + M3$) are characterized by an increased site-scattering value with respect to that of the prismatic fluoro-edenite (Table 8). This increase is consistent with the site distribution inferred from

TABLE 7. EXPERIMENTAL DETAILS OF THE COLLECTION OF X-RAY POWDER-DIFFRACTION DATA AND MISCELLANEOUS DATA ABOUT THE REFINEMENT

Instrument	Siemens D5005
X-ray tube	Cu at 40 kV and 40 mA (Cu$K\alpha_1$ = 1.540598 Å)
Incident beam optic	Multilayer X-ray mirrors
Sample mount	Rotating capillary (30 rpm)
Soller slits	2 (2.3° divergence)
Divergence and antidivergence slits	1 mm
Detector slit	0.2 mm (0.1°)
Detector	Solid state Si(Li) SolX
2θ range (°)	3–120 (5851 data points)
Step size (°)	0.02
Counting time (s)	30
R_p (%), R_{wp} (%), R_F (%)	5.14, 6.78, 4.43
Reduced χ^2	1.170
Durbin–Watson D statistic	1.760
Restraints contribution to χ^2	73.5
Refined parameters	99
Peak cut-off (%)	0.02
J	1.036
GV, GW	19(4), 6.8(7)
LY	20.8(8)
S/L = H/L	0.0237(6)
Amphibole wt%	92.44(4)
Albite wt%	7.6(2)

The statistical descriptors are as defined by Young (1993).

TABLE 8. COMPARISON OF UNIT-CELL PARAMETERS AND SITE-SCATTERING VALUES
OBTAINED FROM THE REFINEMENT AND FROM AVERAGED CHEMICAL COMPOSITION

	Fibrous fluoro-edenite (present work)			Fibrous amphibole [a]	Prismatic Fed [a]	Prismatic Fed [b]
a (Å)	9.8125(3)	-	-	9.815(1)	9.8445(3)	9.846(4)
b (Å)	18.0188(6)	-	-	17.992(3)	18.0091(6)	18.009(6)
c (Å)	5.2781(2)	-	-	5.2733(6)	5.2772(2)	5.277(2)
β (°)	104.620(2)	-	-	104.547(9)	104.813(2)	104.77(2)
V (Å³)	903.00(5)	-	-	901.4(3)	904.50(5)	904.8(5)

	s.s. from refinement	possible site-occupancy	s.s. from site occupancy		s.s. from refinement	s.s. from refinement
O3	**19.4(4)**	$F_{1.970}Cl_{0.020}$	**18.4**	-	**18.8**	**17.95**
A	2.5(10)	$K_{0.157}$	(3.0)	-	0.7	2.51
$A(m)$	3.8(5)	$Na_{0.307}$	(3.4)	-	5.8	5.15
$A2$	-	-	-	-	2.6	0.84
Sum A sites	6.3	-	**6.4**	-	**9.1**	**8.50**
$M4$	37.3(4)	$Ca_{1.505}Na_{0.495}$	(35.6)	-	37.2	37.18
Sum B sites	**37.3**	-	**35.6**	-	**37.2**	**37.18**
$M1$	25.2(4)	$Al_{0.104}Ti_{0.062}$ $Mg_{1.834}$	(24.7)	-	23.4	24.24
$M2$	30.9(4)	$Fe^{3+}_{0.333}Fe^{2+}_{0.125}$ (31.0) $Mn_{0.063}Mg_{1.458}$		-	26.9	27.11
$M3$	12.1(3)	$Fe^{2+}_{0.037}Mg_{0.963}$	(12.5)	-	11.6	12.08
Sum C sites	**68.2**	-	**68.2**	-	**61.9**	**63.43**

Possible site-occupancy is the result of combined data from Mössbauer and Rietveld refinements. Values in parentheses refer to s.s. (site-scattering, in electrons per formula unit) calculated from the possible site-occupancy. For comparison, the data of Gianfagna et al. (2003) for fibrous and prismatic fluoro-edenite (a), and of Gianfagna & Oberti (2001) for prismatic fluoro-edenite (single-crystal analysis) (b), are reported. Fed: fluoro-edenite.

TABLE 9. FRACTIONAL COORDINATES AND ISOTROPIC THERMAL PARAMETERS (NOT REFINED) FOR FIBROUS FLUORO-EDENITE FROM BIANCAVILLA

Site	x	y	z	U_{iso}
O1	0.1115(11)	0.0851(6)	0.2219(21)	0.010
O2	0.1191(12)	0.1727(6)	0.7217(25)	0.010
O3	0.1028(12)	0	0.7077(23)	0.010
O4	0.3670(14)	0.2487(5)	0.7903(28)	0.010
O5	0.3463(14)	0.1344(6)	0.0986(22)	0.010
O6	0.3453(14)	0.1168(6)	0.5959(22)	0.010
O7	0.3425(19)	0	0.2917(37)	0.010
T1	0.2807(8)	0.0838(3)	0.2961(14)	0.005
T2	0.2913(9)	0.1709(3)	0.8047(15)	0.005
M1	0	0.0886(5)	0.5	0.006
M2	0	0.1767(5)	0	0.006
M3	0	0	0	0.006
M4	0	0.2761(4)	0.5	0.011
A	0	0.5	0	0.02
A(m)	0.074(14)	0.5	0.067(21)	0.030

Space group: $C2/m$.

TABLE 10. SELECTED BOND-DISTANCES (Å) FOR FIBROUS FLUORO-EDENITE FROM BIANCAVILLA

		Fibrous Fed	Prismatic Fed			Fibrous Fed	Prismatic Fed
T1	- O1	1.607(10)	1.624(1)	T2	- O2	1.635(10)	1.621(1)
	- O5	1.634(10)	1.645(1)		- O4	1.597(9)	1.589(1)
	- O6	1.660(11)	1.643(2)		- O5	1.646(11)	1.655(2)
	- O7	1.629(7)	1.635(1)		- O6	1.656(10)	1.670(1)
< T1 - O >		1.632	1.637	< T2 - O >		1.633	1.634
M1	- O1 × 2	2.041(10)	2.056(1)	M2	- O1 × 2	2.155(11)	2.152(1)
	- O2 × 2	2.084(10)	2.062(1)		- O2 × 2	2.097(11)	2.080(1)
	- O3 × 2	2.052(1)	2.059(1)		- O4 × 2	2.002(11)	2.003(1)
< M1 - O >		2.059	2.059	< M2 - O >		2.085	2.079
M3	- O1 × 4	2.067(10)	2.055(1)	M4	- O2 × 2	2.367(12)	2.419(1)
	- O3 × 2	2.045(11)	2.029(2)		- O4 × 2	2.298(12)	2.336(1)
< M3-O >		2.060	2.046		- O5 × 2	2.773(12)	2.743(2)
					- O6 × 2	2.574(12)	2.550(2)
< A - O >		2.92	2.915	< M4 - O >		2.503	2.512
< A(m) - O >		2.86	2.863				

The data for prismatic fluoro-edenite (Fed) of Gianfagna & Oberti (2001), obtained by single-crystal analysis, are reported for purposes of comparison.

SEM–EDS chemical data. Increased site-scattering is mainly taken up by the $M2$ site (*ca.* 4 electrons per formula unit, *epfu*) and marginally by $M1$ (*ca.* 1 *epfu*). On the other hand, the <$M4$–O> distance is marginally smaller in the case of the fibers (2.503 Å compared to 2.512 Å of the single crystal) with a comparable site-scattering. In both cases, bond-valence analysis (Brese & O'Keeffe 1991) indicates 1.99 formal charges at the $M4$ sites. However, the crystal-chemical formula of the fibrous amphibole analyzed (Table 5), derived from the average of all the 25 compositions of Table 2, points to a slightly reduced site-scattering with respect to the prismatic fluoro-edenite (*ca.* 1.6 *epfu*). Both <A–O> and <$A(m)$–O> distances gave similar values with respect to the corresponding distances of the prismatic fluoro-edenite. Therefore, according to the structural data, the most important difference between the fibrous and prismatic fluoro-edenite is the significantly reduced site-scattering at the A sites (6.9 with respect to 8.5 *epfu*, respectively). In particular, the reduction is due to a lower Na content, whereas the content of K is comparable. From a combined evaluation of Mössbauer, SEM–EDS and Rietveld refinement data, a reasonable site-distribution pattern may be proposed (Table 8). The $(A + A2)$ site seems to be preferentially occupied by K because of the larger <A–O> bond distance with respect to <$A(m)$–O>. Following the standard site-distribution for amphiboles, $M1$ contains Al and Ti plus Mg, $M2$ contains all Fe^{3+}, part of Fe^{2+} and Mg, $M3$ hosts the remaining Fe^{2+} and Mg, and $M4$ contains Mn, Ca and Na.

As observed in Figure 3, the compositional spread of the Biancavilla fibers is larger than that of the prismatic fluoro-edenite. Even though three compositions fall in the fields of tremolite, six in that of winchite, and only one in that of richterite, fifteen compositions fall in the edenite field, corresponding to about 65% of the total analyzed fibers. If we consider the mean crystal-chemical formula obtained by the average of the 25 analyses, we obtain: $(Na_{0.307}K_{0.157})_{\Sigma 0.464} (Ca_{1.505}Na_{0.495})_{\Sigma 2.000}$ $(^{VI}Al_{0.104}Fe^{3+}_{0.333}Fe^{2+}_{0.162}Mg_{4.255}Ti_{0.062}Mn_{0.063})_{\Sigma 4.980}$ $(Si_{7.520}{}^{IV}Al_{0.480})_{\Sigma 8.000} O_{22} (F_{1.970}Cl_{0.020})_{\Sigma 1.990}$. The minimum and maximum *apfu* values obtained from all the 25 analyses are reported in Table 5.

CONCLUSIONS

In light of the multianalytical approach adopted here to characterize the Biancavilla fibrous amphibole, we have found that: a) the cell volume is reduced with respect to the prismatic fluoro-edenite, owing to smaller occupancy of the A site; b) the Fe^{3+}/Fe_{tot} ratio is lower in the fibers; c) Fe^{3+} is exclusively present at the $M2$ site, whereas Fe^{2+} is distributed between the $M2$ and $M3$ sites, in agreement with the cation distribution proposed by Gunter *et al.* (2003).

The marked differences in both total Fe content and site partitioning between the fibrous and prismatic

fluoro-edenite suggest that they had a different genetic history. A genetic hypothesis was already proposed for these F-rich amphiboles by Gianfagna & Oberti (2001) and Gianfagna *et al.* (2003): a hot fluid, enriched in F and other incompatible elements emanating from the cooling benmoreitic magma, was responsible for the alteration and metasomatism of the original benmoreitic rocks. The results obtained in the present work allow us to make some specific considerations: 1) the higher Fe content of the fibers is consistent with their later crystallization with respect to the prismatic fluoro-edenite; 2) the fibrous morphology and the higher content of Fe^{2+} in the fibers respect to the prismatic fluoro-edenite support an extremely rapid crystallization, in which the Fe did not have enough time to be oxidized, and the fibers did not increase in diameter.

As a result of *in vitro* and *in vivo* experiments already performed, Cardile *et al.* (2004) and Soffritti *et al.* (2004) found that the prismatic fluoro-edenite, even where previously pulverized, is not as reactive as the fibrous variety. Our results indicate that this may be due not only to the fibrous morphology, but also to the highest content of Fe^{2+}, which is more reactive than Fe^{3+} in organic environments (*i.e.,* the lungs). This is still a very interesting and open issue, to be investigated from a biomedical perspective.

REFERENCES

ANDREOZZI, G.B., LUCCHESI, S., GRAZIANI, G. & RUSSO, U. (2004): Site distribution of Fe^{2+} and Fe^{3+} in the axinite mineral group: new crystal-chemical formula. *Am. Mineral.* **89**, 1763-1771.

BANDLI, B.R., GUNTER, M.E., TWANLEY, B., FOIT, F.F., JR. & CORNELIUS , S.B. (2003): Optical, compositional, morphological, and x-ray data on eleven particles of amphiboles from Libby, Montana, Usa. *Can. Mineral.* **41**, 1241-1253.

BRESE, N.E. & O'KEEFFE, M. (1991): Bond-valence parameters for solids. *Acta Crystallogr.* **B47**, 192-197.

BURRAGATO, F., COMBA, P., BAIOCCHI, V., PALLADINO, D.M., SIMEI, S., GIANFAGNA, A., PAOLETTI, L. & PASETTO, R. (2005): Geo-volcanological, mineralogical and environmental aspects of quarry materials related to pleural neoplasm in the area of Biancavilla, Mount Etna (eastern Sicily, Italy). *Environ. Geol.* **47**, 855-868.

CARDILE, V., RENIS, M., SCIFO, C., LOMBARDO, L., GULINO, R., MANCARI, B. & PANICO, AM. (2004): Behaviour of new asbestos amphibole fluoro-edenite in different lung cell systems. *Int. J. Biochem. Cell Biol.* **36**, 849-860.

COMBA, P., GIANFAGNA, A. & PAOLETTI, L. (2003): The pleural mesothelioma cases in Biancavilla are related to the new fibrous amphibole fluoro-edenite. *Arch. Environ. Health* **58**, 229-232.

DUNCAN, A.M. (1976): Pyroclastic flow deposits in the Adrano area of Mount Etna, Sicily. *Geol. Mag.* **113**, 357-363.

DYAR, M.D., MACKWELL, S.M., MCGUIRE, A.V., CROSS, L.R. & ROBERTSON, J.D. (1993): Crystal chemistry of Fe^{3+} and H^+ in mantle kaersutite: implications for mantle metasomatism. *Am. Mineral.* **78**, 968-979.

FINGER, L.W., COX, D.E. & JEPHCOAT, A.P. (1994): A correction for powder diffraction peak asymmetry due to axial divergence. *J. Appl. Crystallogr.* **27**, 892-900.

GIANFAGNA, A., BALLIRANO, P., BELLATRECCIA, F., BRUNI, B.M., PAOLETTI, L. & OBERTI, R. (2003): Characterization of amphibole fibres linked to mesothelioma in the area of Biancavilla, eastern Sicily, Italy. *Mineral. Mag.* **67**, 1221-1229.

GIANFAGNA, A. & OBERTI, R. (2001): Fluoro-edenite from Biancavilla (Catania, Sicily, Italy): crystal chemistry of a new amphibole end-member. *Am. Mineral.* **86**, 1489-1493.

GOLDMAN, D.S. (1979): A reevaluation of the Mössbauer spectroscopy of calcic amphiboles. *Am. Mineral.* **64**, 109-118.

GUNTER, M.E., DYAR, M.D., TWAMLEY, B., FOIT, F.F. & CORNELIUS, C. (2003): Composition, $Fe^{3+}/\Sigma Fe$, and crystal structure of non-asbestiform and asbestiform amphiboles from Libby, Montana, U.S.A. *Am. Mineral.* **88**, 1970-1978.

LAGAREC, K. & RANCOURT, D.G. (1998): RECOIL, Mössbauer Spectral Analysis Software for Windows (version 1.0). Department of Physics, University of Ottawa, Canada.

LARSON, A.C. & VON DREELE, R.B. (1985): General Structure Analysis System (GSAS). *Los Alamos Nat. Lab. Rep.* **LAUR 86-748**.

LEAKE, B.E., WOOLLEY, A.R., ARPS, C.E.S., BIRCH, W.D., GILBERT, M.C., GRICE, J.D., HAWTHORNE, F.C., KATO, A., KISCH, H.J., KRIVOVICHEV, V.G., LINTHOUT, K., LAIRD, J., MANDARINO, J.A., MARESH, V.W., NICKEL, E.H., ROCK, N.M.S., SCHUMACHER, J.C., SMITH, D.C., STEPHENSON, N.N., UNGARETTI, L., WHITTAKER, E.J.W. & GUO, YOUZHI (1997): Nomenclature of amphiboles: report of the Subcommittee on Amphiboles of the International Mineralogical Association, Commission on New Minerals and Mineral Names. *Can. Mineral.* **35**, 219-246.

LONG, G.J., CRANSHAW, T.E. & LONGWORTH, G. (1983): The ideal Mössbauer effect absorber thickness. *Mössbauer Effect Reference Data J.* **6**, 42-49.

MEEKER, G.P., BERN, A.M., BROWNFIELD, I.K., LOWERS, H.A., SUTLEY, S.J., HOEFEN, T.M. & VANCE, J.S. (2003): The composition and morphology of amphiboles from the Rainy Creek Complex, near Libby, Montana. *Am. Mineral.* **88**, 1955-1969.

MENEGHINELLO, E., ALBERTI, A. & CRUCIANI, G. (1999): Order–disorder process in the tetrahedral sites of albite. *Am. Mineral.* **84**, 1144-1151.

OBERTI, R., UNGARETTI, L., CANNILLO, E. & HAWTHORNE, F.C. (1992): The behaviour of Ti in amphiboles. I. Four- and six-coordinate Ti in richterite. *Eur. J. Mineral.* **4**, 425-439.

PAOLETTI, L., BATISTI, D., BRUNO, C., DI PAOLA, M., GIANFAGNA, A., NESTI, M. & COMBA, P. (2000): Unusually high incidence of malignant pleural mesothelioma in a town of eastern Sicily: an epidemiological and environmental study. *Arch. Environm. Health* **55**, 392-8.

RANCOURT, D.G. (1994a): Mössbauer spectroscopy of minerals. I. Inadequacy of Lorentzian-line doublets in fitting spectra arising from quadrupole splitting distributions. *Phys. Chem. Minerals* **21**, 244-249.

RANCOURT, D.G. (1994b): Mössbauer spectroscopy of minerals. II. Problem of resolving cis and trans octahedral Fe^{2+} sites. *Phys. Chem. Minerals* **21**, 250-257.

RANCOURT, D.G. & PING, J.Y. (1991): Voigt-based methods for arbitrary-shape static hyperfine parameter distributions in Mössbauer spectroscopy. *Nucl. Instrum. Methods Phys. Res.* **B58**, 85-97.

ROMANO, R. (1982): Succession of the volcanic activity in the Etnean area. *Soc. Geol. Ital., Mem.* **23**, 27-48.

SCHMIDBAUER, E., KUNZMANN, T., FEHR, T. & HOCHLEITNER, R. (2000): Electrical resistivity and ^{57}Fe Mössbauer spectra of Fe-bearing calcic amphiboles. *Phys. Chem. Minerals* **27**, 347-356.

SOFFRITTI, M., MINARDI, F., BUA, L., DEGLI ESPOSTI, D. & BELPOGGI, F. (2004): First experimental evidence of peritoneal and pleural mesotheliomas induced by fluoro-edenite fibres in Etnean volcanic material from Biancavilla (Sicily, Italy). *Eur. J. Oncol.* **9**, 169-175.

THOMPSON, P., COX, D.E. & HASTINGS, J.B. (1987): Rietveld refinement of Debye–Scherrer synchrotron X-ray data from Al_2O_3. *J. Appl. Crystallogr.* **20**, 79-83.

TOBY, B.H. (2001): EXPGUI, a graphical user interface for GSAS. *J. Appl. Crystallogr.* **34**, 210-213.

VON DREELE, R.B. (1997): Quantitative texture analysis by Rietveld refinement. *J. Appl. Crystallogr.* **30**, 517-525.

WYLIE, A. & VERKOUTEREN, J. (2000): Amphibole asbestos from Libby, Montana: aspects of nomenclature. *Am. Mineral.* **85**, 1540-1542.

YOUNG, R.A. (1993): Introduction to the Rietveld method. *In* The Rietveld Method (R.A. Young, ed.). Oxford University Press, Oxford, U.K. (1-38).